

# ARMAS: Active Reconstruction of Missing Audio Segments

Zohra Cheddad

*Département de Mathématiques*

*Université Frères Mentouri I*

Constantine, Algeria

zcheddad929@gmail.com

Abbas Cheddad

*Department of Computer Science*

*Blekinge Institute of Technology*

Karlskrona, Sweden

abbas.cheddad@bth.se / 0000-0002-4390-411X

**Abstract**—Digital audio signal reconstruction of a lost or corrupt segment using deep learning algorithms has been explored intensively in recent years. Nevertheless, prior traditional methods with linear interpolation, phase coding and tone insertion techniques are still in vogue. However, we found no research work on reconstructing audio signals with the fusion of dithering, steganography, and machine learning regressors. Therefore, this paper proposes the combination of steganography, halftoning (dithering), and state-of-the-art shallow (RF- Random Forest regression) and deep learning (LSTM- Long Short-Term Memory) methods. The results (including comparing the SPAIN, Autoregressive, deep learning-based, graph-based, and other methods) are evaluated with three different metrics. The observations from the results show that the proposed solution is effective and can enhance the reconstruction of audio signals performed by the side information (e.g., Latent representation and learning for audio inpainting) steganography provides. Moreover, this paper proposes a novel framework for reconstruction from heavily compressed embedded audio data using halftoning (i.e., dithering) and machine learning, which we termed the HCR (halftone-based compression and reconstruction). This work may trigger interest in optimising this approach and/or transferring it to different domains (i.e., image reconstruction). Compared to existing methods, we show improvement in the inpainting performance in terms of signal-to-noise (SNR), the objective difference grade (ODG) and the Hansen’s audio quality metric.

**Index Terms**—Audio Reconstruction, Halftoning, Steganography, Machine learning.

## I. INTRODUCTION

Corrupt audio files and lost audio transmission and signals are severe issues in several audio processing activities such as audio enhancement and restoration. For example, in different applications and music enhancement and restoration situations, gaps could occur for several seconds [1]. Audio signal reconstruction remains a fundamental challenge in machine learning and deep learning despite the remarkable recent development in neural networks [1]. Audio in-painting, audio interpolation/extrapolation, or waveform replacement address the restoration of lost information in audio. The reconstruction aims to provide consistent and relevant information while eliminating audible artefacts to keep the listener unaware of any occurring issues [2]. The active reconstruction can be considered a preemptive security measure to allow for self-healing when part of the audio becomes corrupted. Active reconstruction means reconstructing lost signals by incorporat-

ing side information retrieved from pre-embedded data. Thus, the technique is not intended for any degraded audio but only for audio protected by the steganography information. To this end, and to the best of our knowledge, we found no prior research work on the active reconstruction of audio signals with the fusion of steganography (an information hiding technique), halftoning and machine learning (ML) models. The initial idea (without ML) was proposed in a PhD thesis as an application of steganography. The hiding strategy of steganography can be tailored to act as an intelligent streaming audio/video system that uses techniques to conceal transmission faults from the listener that are due to lost or delayed packets on wireless networks with bursty arrivals; thus, providing a disruption tolerant broadcasting channel [3].

## II. RELATED WORK

In the work of Khan et al. [4], the authors proposed a modern neuro-evolution algorithm, Enhanced Cartesian Genetic Programming Evolved Artificial Neural Network (ECGPANN), as a predictor of the lost signal samples in real-time. The authors have trained and tested the algorithms on audio speech signal data and evaluated them on the music signal. A deep neural network (DNN)-based regression method was proposed in [5] for a packet loss concealment (PLC) algorithm to predict a missing frame’s characteristics. Two other DNNs were developed for the training by integrating the log-power spectra and phases based on the unsupervised pre-training and supervised fine-tuning. The algorithm then provides the previous frame features to the trained DNN to reconstruct the missing frames. In [1], researchers have analyzed audio gaps (500 - 550 ms) and used Wasserstein Generative Adversarial Network (WGAN) and Dual Discriminator WGAN (D2WGAN) models to reconstruct the lost audio content. In Khan et al. [6], the authors proposed an audio signal reconstruction model called Cartesian Genetic Programming evolved Artificial Neural Network (CGPANN), which was more efficient than the interpolation-extrapolation techniques. The developed model was robust in recovering signals contaminated with up to 50% noise. In [2], the authors proposed a DNN structure to restore the missing audio content based on the audio gaps. The signals provided in the audio gaps in the DNN structure were time-frequency

coefficients (either complex values or magnitude). In the work of Sperschneider et al. [7], the authors presented a delay-less packet-loss concealment (PLC) method for stationary tonal signals, which addresses audio codecs that utilizes a modified discrete cosine transformation (MDCT). In the case of a frame loss, tonal components are identified using the last two obtained spectra and their pitch information. Furthermore, the MDCT coefficients of the tonal components were estimated using phase prediction based on the detection of tonal components. Mokrý et al. [8] presented an inpainting algorithm called SPAIN (SParse Audio INpainter) developed by an adaptation of the successful declipping method, SPADE [9], to the context of audio inpainting. The authors show that the analysis of their algorithm, SPAIN, performs the best in terms of SNR (signal-to-noise ratio) among sparsity-based methods and reaches results on a par with the state-of-the-art Janssen algorithm [10]<sup>1</sup> for audio inpainting. A composite model for audio enhancement that combines the Long Short-Term Memory (LSTM) and the Convolutional Neural Network (CNN) models was proposed in [11]. Perraudin et al. [12], proposed a reconstruction method for the loss of long signals in audio (i.e., Music signals). The concealment of such signal defects is based on a graph that encodes signal structure in terms of time-persistent spectral similarity and an intuitive optimization embedding scheme. Mokrý and Rajmic [13] proposed a heuristic method for compensating for energy loss after running the  $\mathcal{L}_1$  minimization. Their idea is to take the solution and modify it by entrywise multiplication of the recovered gap in the time domain by a compensation curve in order to increase its amplitude; they termed this approach the Time Domain Compensation (TDC) algorithm.

### III. ARMAS: ACTIVE RECONSTRUCTION OF MISSING AUDIO SEGMENTS

Our method aims to reconstruct a realistic segment from audio containing corrupted or dropped regions using active embedding and machine learning. In this section, we describe the proposed method and discuss the individual stages in more detail.

#### A. Halftone-based Compression and Reconstruction (HCR)

In the field of bit-rate reduction, or data compression, the Lempel–Ziv (LZ) or its variant, the Lempel–Ziv–Welch (LZW), are popular methods. However, they are slow and prone to failure if data corruption occurs, as in our case, there were more than 700 samples deleted from the audio signal. Therefore, finding a compression method that is more immune to data corruption and can provide heavy compression and good approximate reconstruction is desired. Hence, the proposed HCR is meant to exploit the halftoning for this purpose. The algorithm this work adapts is that of *Floyd Steinberg*, which applies error forward diffusion [14]. The rationale behind conceiving the notion of HCR is that the

<sup>1</sup>Iteratively fits autoregressive models using a gap’s all previous points for forward estimation and all its future points for backward estimation.

embedding of data in the least significant bits (LSB) of a bit-stream, necessitates dealing with binary data. Let the original audio sampled data be denoted by the vector  $\vec{v} \in \mathbb{R}$ , which is then transformed into a matrix  $\in \mathbb{R}^2$  with suitable dimensions whose automatic estimation is outside of the scope of this work, see equation 1.

$$\vec{v} = ([v_1, v_2, v_3, \dots, v_{j-1}, v_j])^T = D(x, y) = \begin{bmatrix} v_{11} & v_{12} & \dots & v_{1m} \\ v_{21} & v_{22} & \dots & v_{2m} \\ \vdots & \vdots & \ddots & \vdots \\ v_{n1} & v_{n2} & \dots & v_{nm} \end{bmatrix} \quad (1)$$

The matrix  $D(x, y)$  is then passed to the dithering phase using Floyd Steinberg algorithm, which results in a binary matrix (as seen in Fig. 1b) that could be partially inverted. This contributes to the heavy compression that we obtain. For instance, the original audio sampled data and the resulting compressed vector pertaining to Fig. 1b (vectorized), show the following properties: Original Audio (1316019 — **10.04 MB** — Byte) and its corresponding compressed vector (1316019 — **1.26 MB** — Binary), for the length, size and type, respectively.

The error diffusion algorithm exploits the optical system of the human eye which acts as a low-pass filter removing all high frequencies resulting in the illusion of perceiving a dithered image (only binary) as a continuous tone image. Hence, it follows from such notation that in order to partially inverse the dithering operation we need to apply a low-pass filter to attenuate high frequencies (in our case, we choose a 2D Gaussian filter as in Eq. 2 with a kernel size =  $2 \times [2 \times \sigma] + 1$ ).

$$G(x, y) = \frac{1}{2\pi\sigma^2} e^{-\frac{x^2+y^2}{2\sigma^2}} \quad (2)$$

where  $\sigma = 1.50$  (determined heuristically) and  $x, y$  are the coordinates of the image  $D$ . Recently, the development of deep machine learning rekindled interest in addressing the inverse halftoning problem by optimization-based filtering [15] [16]. Nevertheless, we opt to use the simple and computationally-inexpensive method mentioned above.

In order to scrutinize the efficiency of the reconstruction, we calculated the correlation between the original sampled data against the estimated values from the above HCR process. The reconstruction still demonstrates a good correlation  $R = 0.62$ , despite the dithered version constitutes only binary values (either 0 or 1); see Fig. 2. The fitted linear regression model is depicted in Table I. In Fig. 1c, we observe that the process captures a noisy structure and orientation of the original data shown in Fig. 1a; therefore, when this side-information is wedded to machine learning (particularly the state-of-the-art models), it leverages the quality of audio the algorithm reconstructs. This was the impetus for the initiation of this study. To gauge this performance improvement, we tested some ML models whose results appear in section III-B.

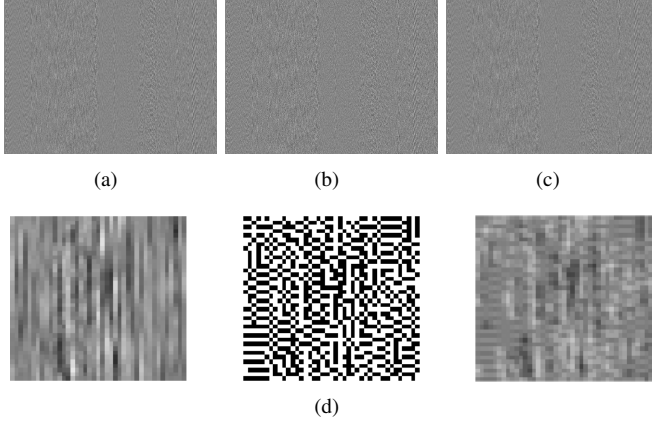


Fig. 1. HCR Visual Inspection: (a) Original audio data reshaped using Eq. 1 and visualised (b) Half-tone of (a) (binary image), (c) Reconstructed (a) from (b) and (d) Small patches cropped from each image left to right, respectively.

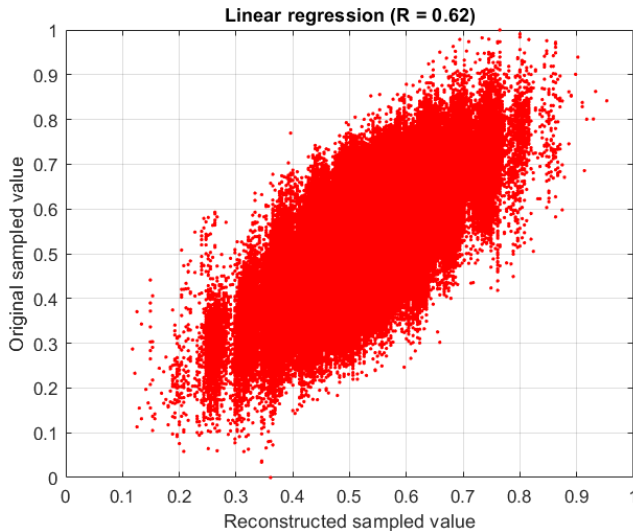


Fig. 2. A dot plot depicting the correlation between the original data and its estimated version. Note that the reconstruction is made from merely binary values (without ML and signal drop).

TABLE I  
EFFECT-ESTIMATES AND  $P$ -values (WALD TESTS) FROM FITTING A LINEAR REGRESSION MODEL FOR THE DATA PLOTTED IN FIG. 1. NUMBER OF OBSERVATIONS: 1316019, ERROR DEGREES OF FREEDOM: 1316017 ROOT MEAN SQUARED ERROR: 0.0527 R-SQUARED: 0.384, ADJUSTED R-SQUARED: 0.384.

	Estimate	SE	tStat	P-value
<b>(Intercept)</b>	0.23791	0.00032051	742.29	0
<b>x1</b>	0.54719	0.00060376	906.3	0

## B. Deployed deep/machine learning architectures

In this section, we list down the different machine learning models we deploy in this study.

1) *Shallow machine learning: Random Forest (RF)* - RF regressor is a supervised decision learning technique for regression that employs the ensemble learning method. The most important parameter is the number of trees which is set to 100 as per the recommendation in the literature [17]. It has been demonstrated that RF is more robust than other similar approaches for handling small samples, high dimensional and nonlinear fitting [18] [19].

2) *Deep machine learning: Long short-term memory (LSTM)* - LSTM is a type of recurrent neural network (RNN) models; it is best suited to make predictions based on time series data by learning long-term dependencies [20]. We have implemented a multi-layer LSTM recurrent neural network to predict the missing signal values with the Keras TensorFlow library (more details in Sec. IV-D).

3) *Training and testing segments:* This section briefly discusses how the two deep/machine learning models are trained and tested. In Fig. 3 (top row), the original audio sampled signal is displayed for mere comparison. Fig. 3 (second row) shows the stego-audio with the embedded copy and a simulation of signal loss (i.e., empty segment). Note that the stego-audio and the original audio look identical since all what was flipped is the last LSB value. Subsequently, we extract the hidden data from the LSB plane, and the values in the extracted binary vector are rearranged by using the same secret key (e.g., for simplicity, we choose the length of the audio segment as the key). The vector is then transformed to a matrix using Eq. (1) (which should correspond to the dithered version), and then a 2D Gaussian filter is applied using Eq. (2). The result is then vectorised to yield the plot shown in Fig. 3 (third row). Part of this vector will be used for training and validation (i.e., the red segments), and the tuned model is finally applied to the test data (i.e., the green segment) to predict (reconstruct) the lost segment. Performing global tuning based on locally adaptive learnt statistics was discussed in previous work though in a different context [21]. Fig. 4, along with the Algorithms (1, 2, 3), provide an in-depth detailed description of our approach. In essence, Alg. 1 describes our embedding approach, while Alg. 2 provides feature extraction based primarily on the extracted embedded data and on its derived augmented feature space using scalogram (namely, the continuous 1-D wavelet transform) [22], which shall form the backbone for the training of the machine learning models.

## IV. PERFORMANCE EVALUATION OF RECONSTRUCTION ALGORITHMS

The experimental samples in this paper are commonly used audio file samples exhibiting different music instruments. As this research focuses on active reconstruction, the audio input is in .wav file format (PCM 16 bit). The main reason for selecting this format is the sound quality, as it preserves the originality of analogue audio without any compression.

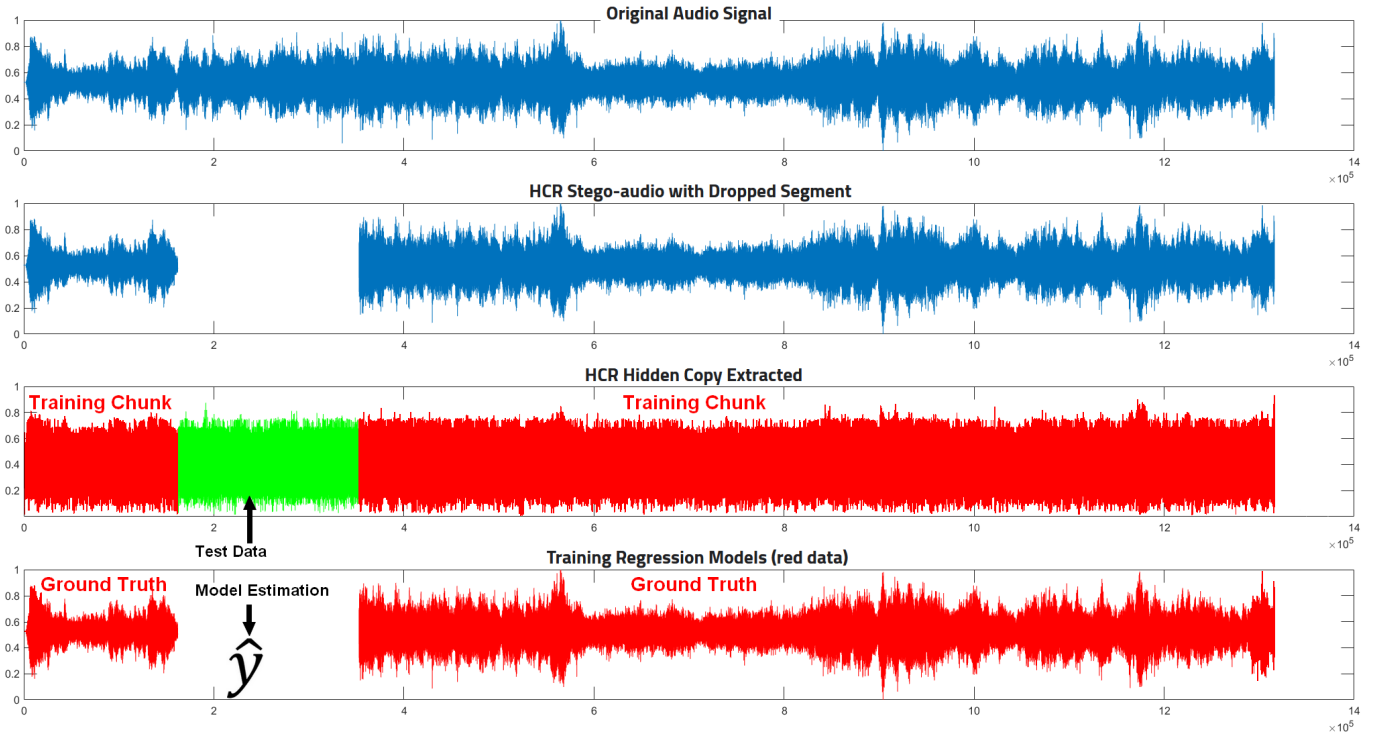


Fig. 3. Audio track segments to train (red) and test (green) machine learning models.

---

#### Algorithm 1: HCR-Embedding Algorithm

---

**Data:** *Audio file S*  
**Result:** *Self-embedded file SS*  
 $S' \leftarrow$  Scale the vector  $S$  to the interval  $[[0,1]*255]$ ;  
 $S'' \leftarrow$  Reshape  $S'$  into a matrix ;  
 /\* dimensions are calculated adaptively \*/  
 $D \leftarrow$  Perform image dithering on  $S''$ ;  
 ; /\* heavy lossy compression \*/  
 $D' \leftarrow$  Flatten  $D$  into a vector;  
 SET SEED  $\alpha = \text{length}(D')$ ;  
 $D'' \leftarrow$  Permute bit stream positions of  $D'$  with  $\alpha$ ;  
 ; /\* to avoid localised distortion \*/  
 $SS \leftarrow$  embed  $D''$  into LSB (least significant bits) of  $S'$ ;  
 $SS \leftarrow$  rescale( $SS$ );  
**Return**  $SS$ ;

---



---

#### Algorithm 2: HCR-Feature Extraction Algorithm

---

**Data:** *Self-embedded file SS with gap G*  
**Result:** *Feature descriptors file F*  
 $S' \leftarrow$  Scale the vector  $SS$  to the interval  $[[0,1]*255]$ ;  
 $S'' \leftarrow$  extract the LSB bit stream of  $S'$ ;  
 SET SEED  $\alpha = \text{length}(S'')$ ;  
 $E \leftarrow$  Invert permutation of the bit stream positions of  $S''$  with  $\alpha$ ;  
 $E' \leftarrow$  Reshape  $E$  into a matrix ;  
 $E'' \leftarrow$  Apply 2D Gaussian filter as in Eq. 2 and flatten it;  
 $W \leftarrow$  Compute scalogram from  $E''$  using continuous 1-D wavelet transform and  $\mathcal{L}_1$  optimisation;  
 $F \leftarrow \text{concat}_{\text{vertically}} \mathfrak{R}(W) \& E''$ ;  
 ; /\* to form the augmented feature space \*/  
**Return**  $F$ ;

---

#### A. State of the Art methods:

The state-of-the-art sparsity-based inpainting techniques to which we compared our approach are the non-learning methods 'ASPAIN' [8], Chambolle-Pock (CP) [23], Douglas-Rachford based (DR) [24], Janssen Autoregressive [10], Orthogonal Matching Pursuit (OMP) [25], 'SSPAIN-H' [8], Revisited and re-weighted methods ('reCP', 'reDR', 'wCP', 'wDR') [13], and the Time Domain Compensation (TDC) [13].

Moreover, we also included a deep-learning based method (D2WGAN) [1] inspired from [26], and a graph-based (Similarity Graphs -SG-) [12]. Our approaches are labeled 'RF', and 'LSTM'. The RF and the LSTM are trained on the extracted pre-embedded data to perform the reconstruction of the missing gap.

#### B. Data set (audio samples):

We used the same audio benchmark as in [8], which comprises 10 files: *Violin, Clarinet, Bassoon, Harp, Glock-*

---

**Algorithm 3: HCR-RF/LSTM Algorithm**

---

**Data:** *Self – embedded file SS with gap G*  
**Data:** *Feature descriptors file F*  
**Result:** *Reconstructed audio file  $\hat{S}$*   
 $M \leftarrow \text{length}(SS)$ ;  
 $N \leftarrow 1$ ;  
 $\text{Train}X \leftarrow []$ ;  
 $\text{Train}Y \leftarrow []$ ;  
 $\text{Test}X \leftarrow []$ ;  
 $\text{Test}Y \leftarrow []$ ;  
**while**  $N \leq M$  **do**  
  **if**  $N \in G$  **then**  
     $\text{Test}X \leftarrow F[N]$ ; /\* Extract features  
      pertaining to the gap G \*/  
  **else**  
    **if**  $N \notin G$  **then**  
       $\text{Train}X \leftarrow F[N]$ ;  
       $\text{Train}Y \leftarrow SS[N]$ ; /\* Response  
      variables are those regions  
      of the uncorrupt signal SS \*/  
    **end**  
  **end**  
**end**  
 $\text{HCRModel} \leftarrow \text{Train RF/LSTM using } \{\text{Train}X,$   
   $\text{Train}Y\}$ ;  
 $\hat{G} \leftarrow \text{HCRModel } \{\text{Test}Y\}$ ; /\* Estimate the  
  gap using the trained model \*/  
 $\hat{S} \leftarrow SS + \hat{G}$ ;  
**Return**  $\hat{S}$

---

*enspie, Celesta, Accordion, Guitar sarasate, Piano schubert, and Wind ensemble stravinsky*. The gap length of 100 ms and 300 ms were chosen randomly from the set so that the gaps do not overlap. Therefore, we ran a total of 280 tests ( $14(\text{methods}) \times 10(\text{segments}) \times 2(\text{gaps})$ ). These tests (Phase I) were run on all methods reported in the previous section except the D2WGAN and SG.

In the second stage (Phase II), we deploy the deep learning and the SG methods. We first select the top-performing methods from Phase I. Then, we perform additional tests using the *Piano* and the *Acoustic Guitar and Orchestra* (Mixed instruments) audio files, the gaps' length of 520 ms, 820 ms, 865ms, and 883ms were chosen following the paper [1].

### C. Evaluation metrics:

We utilise three commonly used reference-based metrics to evaluate the performance of the different audio restoration algorithms. The first is the objective difference grade (ODG) which is described in the Perceptual Evaluation of Audio Quality (PEAQ) standard algorithm used for objective measurements of perceived audio quality. It is believed to be based on generally accepted psycho-acoustic principles that approximate the subjective difference grade used in human-based audio tests [27] [28] [29]. The second is related to

ODG but uses Hansen's method and a different model for speech quality estimation [30]; this metric is termed herein "QC". The third standard performance measure is the signal-to-noise ratio (SNR), defined as follows:

$$\text{SNR}(S, \hat{S}) = 10 \cdot \log_{10} \frac{\|S\|_2^2}{\|S - \hat{S}\|_2^2} \quad (3)$$

where  $S$  is the original signal,  $\hat{S}$  is the reconstructed signal (an estimate of  $S$ ).

All of the metrics capture objective measures of signal quality. The ODG metric's values range from 0.0 (imperceptible audio distortion) to -4.0 (very annoying distortion). The SNR is measured in dB (decibel); the higher it is, the better the reconstructed signal is. The objective speech quality measure (QC) would ideally reach to 1.000 with a perfect reconstruction.

### D. Software environment:

The RF and other algorithms are executed using MATLAB (R2022a); for the LSTM implementation, we used Python (Keras, Pandas, Scipy, Numpy and TensorFlow libraries). The LSTM properties are as follows: model (Sequential()), Dropout (0.2), Optimizer (Adam), learning rate (0.0001), and the loss function for our model was measured using MSE (mean squared error). Finally, we fit the models with a batch size of 32 and 40 epochs (to avoid overfitting, as the training process had a stable loss within the first five iterations).

## V. RESULTS AND DISCUSSION

The comparison is performed between the original and the reconstructed audio signals in this study. After extracting the required training data from the sequence (see Fig. 4), the data is then augmented using a scalogram. The aggregated data (features) are then passed to RF and LSTM models for training; see Algorithm 2. The test set is the hidden data embedded in the stego-audio whose dynamic range is extended using 2D Gaussian filter and whose feature space is extended using the scalogram; see Algorithms 2 and 3. The evaluation of the reconstructed signals to the original signal (which acts as the reference for validation) is observed by calculating the statistical metrics reported above. Many state-of-the-art audio inpainting algorithms (in Phase I) had their performance deteriorating when exceeding the range of very short gaps ( $\approx 45\text{ms}$ ); see Fig. 5 where we show a visual summary of the performance with gaps of 100ms and 300ms (20 tests for each method). In Phase II, we observed good performance of the proposed approach for more extended gap reconstruction (e.g., 800ms). Fig. 6 depicts a ranking summary, and Fig. 7 shows a real example of an audio gap reconstruction whose blow-up is presented in Fig. 8, allowing closer scrutiny of the reconstruction quality. Additional example is furnished online <sup>2</sup>. Moreover, the ability to handle lengthy missing gaps (e.g., 4000ms, 8000ms) teases our approach apart from other methods. The already existing methods, which we examined,

<sup>2</sup>Audio Clips (medium gaps): <https://ardisdataset.github.io/ARMAS2/>

TABLE II

AVERAGE RANKING OF THE DIFFERENT METHODS IN PHASE II (8 TESTS) MEASURED USING THE THREE AUDIO QUALITY METRICS. ODG AND SNR ARE DEPICTED GRAPHICALLY IN FIG. 6.

Method	Rank-ODG	Rank-QC	Rank-SNR
<b>Proposed-LSTM</b>	2.50	2.50	4.00
<b>Proposed-RF</b>	2.50	2.00	1.25
<b>wCP [23]</b>	3.50	5.25	4.75
<b>D2WGAN [1]</b>	4.00	2.75	5.50
<b>SG [12]</b>	5.25	5.75	4.25
<b>SPAIN [8]</b>	5.25	4.50	4.50
<b>TDC [13]</b>	5.50	5.50	3.75

are not designed nor able to handle these large gaps' reconstruction. The audio files of our experiments (i.e., LSTM, RF) are available online <sup>3</sup>. The experiments reinforce that deep learning reconstruction approaches can benefit from embedded side information if designed carefully, compare D2WGAN to our approaches in Fig. 6 and Table. II.

## VI. CONCLUSIONS

The aim of this paper is to put forward a new framework which proposes the fusion of audio dither-based steganography with machine/deep learning for the active reconstruction of lost signals. The results show that the proposed solution is feasible and can enhance the reconstruction of lost audio signals (readers may wish to listen to the audio online, see URL in section V). We conducted experiments on several types of signal drops of [100ms, 300ms], [500ms to 800ms] and [4000ms, 8000ms (shown online)]. As a proof-of-concept, we can assert that, in general, the LSTM and the RF models are good models to utilise. Our approach is not meant to replace current inpainting audio methods but rather to assist them by providing latent side information. It can also benefit security systems in protecting audio files from unauthorised manipulation. The contribution of this work is twofold: —A halftone-based compression and reconstruction (HCR) —Orchestration of the three scientific disciplines: steganography, compression and audio processing. The paper supplies extensive experiments, which we believe are compelling evidence of the efficacy of our proposed approach, a corollary when combining halftoning, steganography and machine learning. To our knowledge, we found no similar implementation in the literature for audio missing-segment reconstruction. Thus, we conclude this paper by stating that the fusion of steganography and state-of-the-art machine learning algorithms can be considered for the active reconstruction of audio signals. However, as we pointed out in the discussion section, there is room for enhancement, for example, enhancing the algorithm for inverse-halftoning, which is an ill-posed problem.

## ACKNOWLEDGMENT

We thank the reviewers for their neutrality in assessing this manuscript and for the constructive feedback.

<sup>3</sup>Audio Clips (lengthy gaps): <https://ardisdataset.github.io/ARMAS/>

## REFERENCES

- [1] P. P. Ebner and A. Eltelt, "Audio inpainting with generative adversarial network," arXiv preprint arXiv:2003.07704, 2020.
- [2] A. Marafioti, N. Perraudin, N. Holighaus, and P. Majdak, "A context encoder for audio inpainting," *IEEE/ACM Transactions on Audio, Speech, and Language Processing*, vol. 27, no. 12, pp. 2362–2372, 2019.
- [3] A. Cheddad, "Steganoflage: A New Image Steganography Algorithm," School of Computing and Intelligent Systems, Faculty of Computing and Engineering, University of Ulster, United Kingdom, September, 2009.
- [4] G. M. Khan and N. M. Khan, "Real-time lossy audio signal reconstruction using novel sliding based multi-instance linear regression/random forest and enhanced cgpann," *Neural Processing Letters*, pp. 1–29, 2020.
- [5] B.-K. Lee and J.-H. Chang, "Packet loss concealment based on deep neural networks for digital speech transmission," *IEEE/ACM Transactions on Audio, Speech, and Language Processing*, vol. 24, no. 2, pp. 378–387, 2015.
- [6] N. M. Khan and G. M. Khan, "Audio signal reconstruction using cartesian genetic programming evolved artificial neural network (CGPANN)," in 2017 16th IEEE International Conference on Machine Learning and Applications (ICMLA). IEEE, 2017, pp. 568–573.
- [7] R. Sperschneider, J. Sukowski, and G. Marković, "Delay-less frequency domain packet-loss concealment for tonal audio signals," in 2015 IEEE Global Conference on Signal and Information Processing (GlobalSIP). IEEE, 2015, pp. 766–770.
- [8] O. Mokry, P. Závíska, P. Rajmic and V. Vesely, "Introducing SPAIN (SParse Audio INpainter)," 2019 27th European Signal Processing Conference (EUSIPCO), 2019, pp. 1-5, doi: 10.23919/EUSIPCO.2019.8902560.
- [9] S. Kitic, N. Bertin, and R. Gribonval, "Sparsity and cosparsity for audio declipping: A flexible non-convex approach," In Proc: 12th International Conference on Latent Variable Analysis and Signal Separation, Aug 2015, Liberec, Czech Republic.
- [10] A. J. E. M. Janssen, R. N. J. Veldhuis, and L. B. Vries, "Adaptive interpolation of discrete-time signals that can be modeled as autoregressive processes," *IEEE Trans. Acoustics, Speech and Signal Processing*, vol. 34, no. 2, pp. 317–330, 1986.
- [11] M. Hasannezhad, W.-P. Zhu, and B. Champagne, "A novel low-complexity attention-driven composite model for speech enhancement," in 2021 IEEE International Symposium on Circuits and Systems (ISCAS). IEEE, 2021, pp. 1–5.
- [12] N. Perraudin, N. Holighaus, P. Majdak and P. Balazs, "Inpainting of Long Audio Segments With Similarity Graphs," in *IEEE/ACM Transactions on Audio, Speech, and Language Processing*, vol. 26, no. 6, pp. 1083-1094, June 2018, doi: 10.1109/TASLP.2018.2809864.
- [13] O. Mokry and P. Rajmic, "Audio Inpainting: Revisited and Reweighted," in *IEEE/ACM Transactions on Audio, Speech, and Language Processing*, vol. 28, pp. 2906-2918, 2020, doi: 10.1109/TASLP.2020.3030486.
- [14] R.W. Floyd, and L. Steinberg, "An Adaptive Algorithm for Spatial Greyscale," In: *Proceedings of the Society of Information Display*, vol(17)(2), pp. 75-77, 1976.
- [15] T.H. Kim, Tae-Hoon, S.I. Park, "Deep context-aware descreening and rescreening of halftone images". *ACM Transactions on Graphics*, vol. 37, no. 4, pp. 1–12, 2018.
- [16] Y. Li, J.B. Huang, N. Ahuja, M.H. Yang, "Deep Joint Image Filtering." In: B. Leibe, J. Matas, N. Sebe, M. Welling. (eds) *Computer Vision – ECCV'16*. 2016. Lecture Notes in Computer Science, vol 9908. Springer, Cham.
- [17] S.K. Dasari, A. Cheddad, P. Andersson, "Random Forest Surrogate Models to Support Design Space Exploration in Aerospace Use-Case," In: MacIntyre J., Maglogiannis I., Iliadis L., Pimenidis E. (eds) *Artificial Intelligence Applications and Innovations. AIAI 2019. IFIP Advances in Information and Communication Technology*, vol 559. Springer, Cham.
- [18] S.K. Dasari, A. Cheddad, and P. Andersson, "Predictive modelling to support sensitivity analysis for robust design in aerospace engineering," *Structural and Multidisciplinary Optimization* (2020), pp. 1–16.
- [19] Raquel Espinosa, José Palma, Fernando Jiménez, Joanna Kamińska, Guido Sciacvico, Estrella Lucena-Sánchez, "A time series forecasting based multi-criteria methodology for air quality prediction," *Applied Soft Computing* 113 (2021) 107850.
- [20] L. Sun, J. Du, L. Dai, and C. Lee, "Multiple-target deep learning for LSTM-RNN based speech enhancement," In Proc: *Hands-free Speech Communications and Microphone Arrays (HSCMA'17)*, pp. 136-140. IEEE, San Francisco (2017).



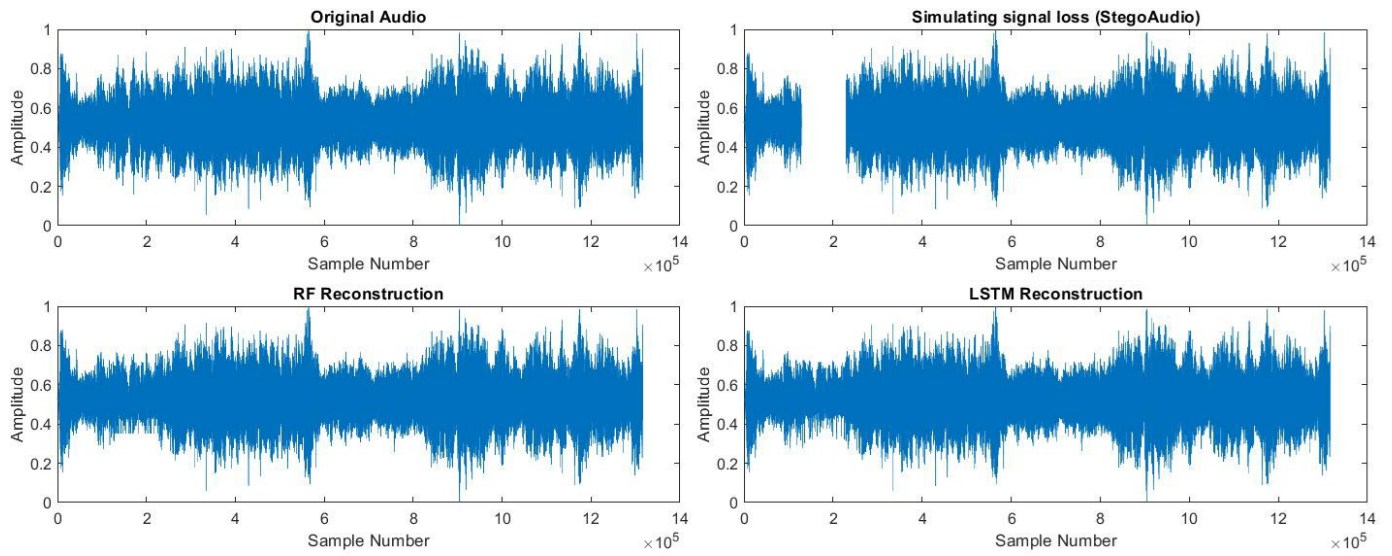


Fig. 4. Reconstruction of a short audio signal using RF and LSTM.

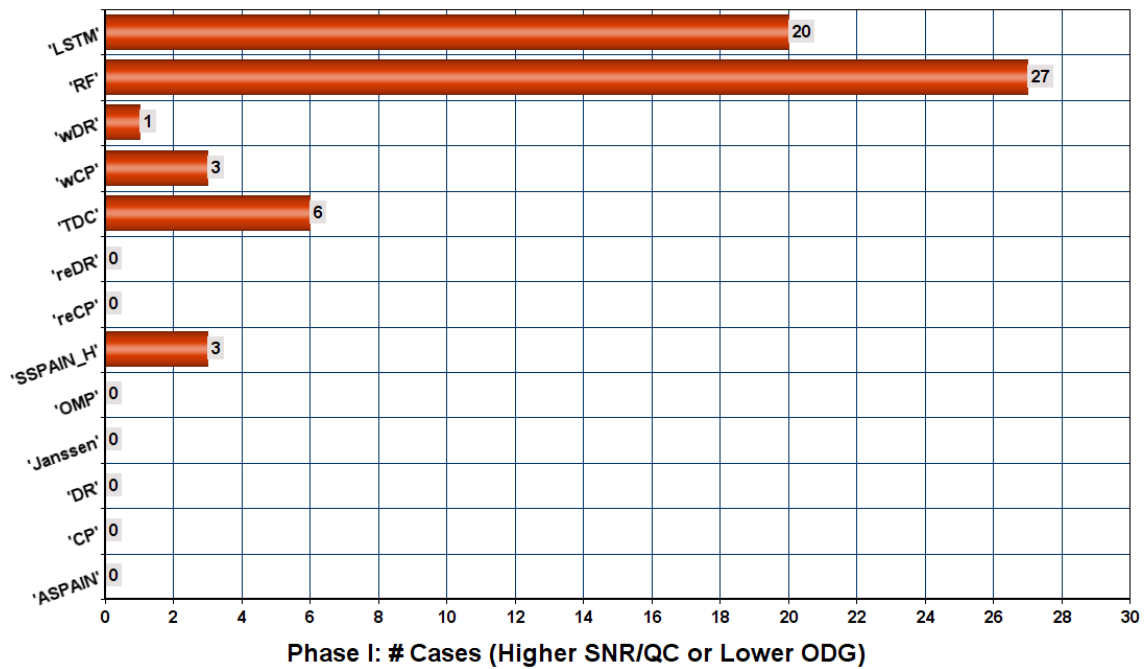


Fig. 5. Phase I: Determining the best performing non-learning methods. From the results of 20 tests on each of these methods, we have two competitive methods (CP and TDC) that will be tested in Phase II. Although ASPAIN has had no winning cases, since it is a recent algorithm, we opt to pass it to phase II (see subsection IV-B). The *X-axis* denotes the number of cases in which a given algorithm outperformed others in SNR or ODG (20 tests were measured). Detailed numerical results, on which this figure is based, are furnished in the supplementary files.

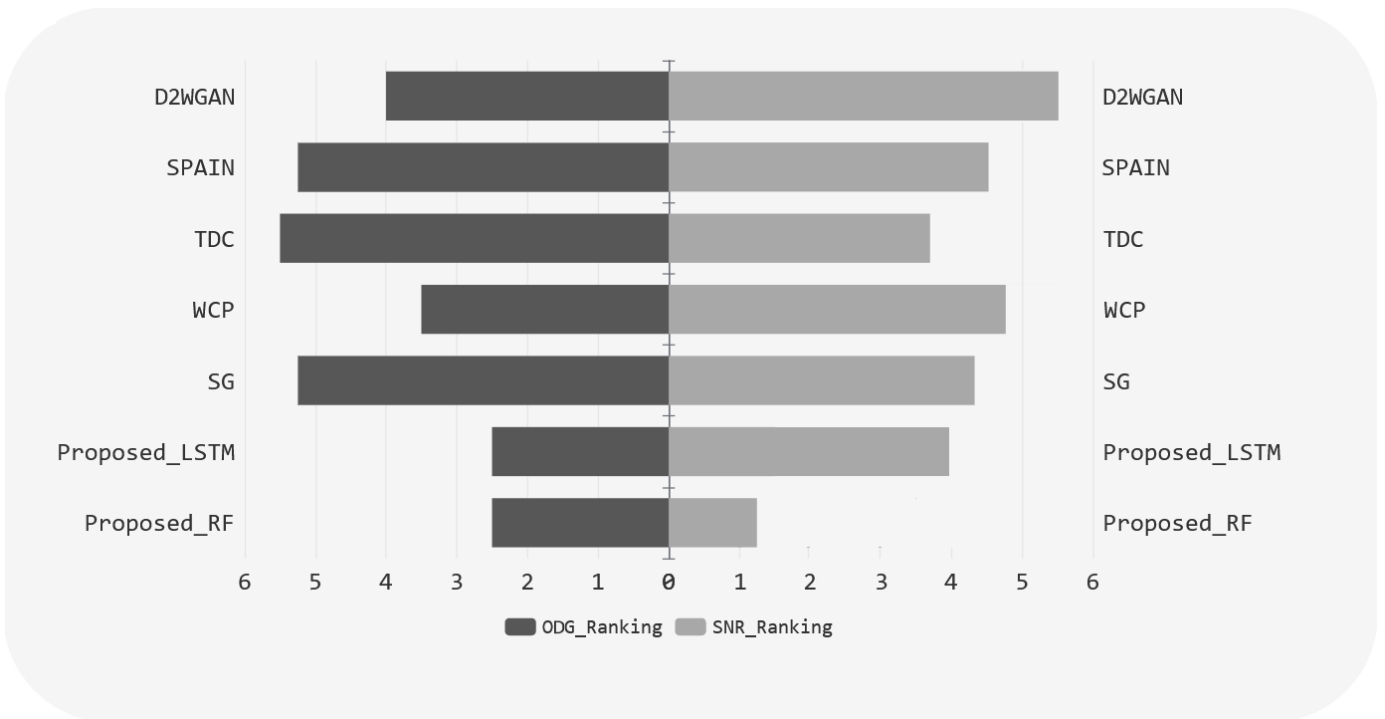


Fig. 6. Phase II: Determining the best-performing methods, including deep learning-based (D2WGAN) and graph-based (SG). From the results of 8 tests on each of these methods, we can observe that RF and LSTM (sequence-to-sequence modelling) exhibit promising results on both metrics (SNR and ODG), which ranked them at the top of the list. Detailed numerical results, on which this figure is based, are furnished in the supplementary files.

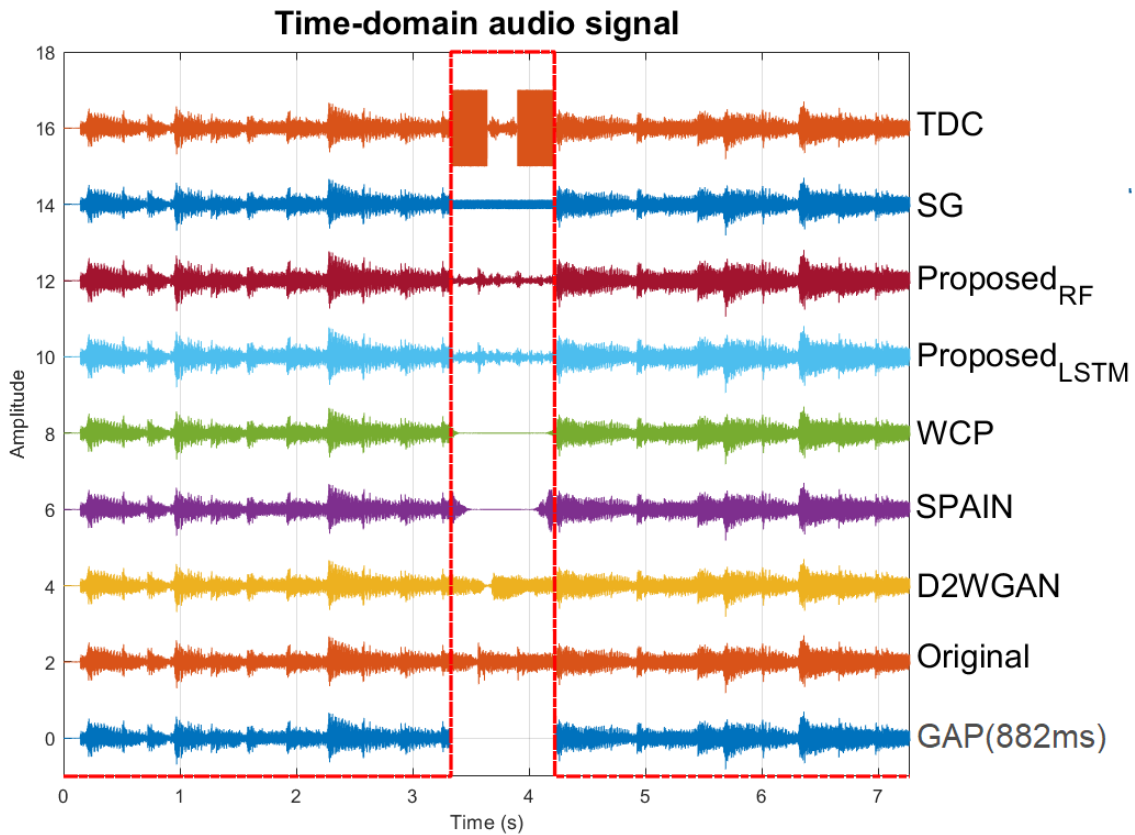


Fig. 7. Phase II - Audio reconstruction test-: Performance of the different audio inpainting algorithms on an example audio sample (*extend-solo-1-real-36*) [1]. The GAP signal is merely the Original audio sample but with the gap (highlighted in red dashed line) simulating dropped signal.



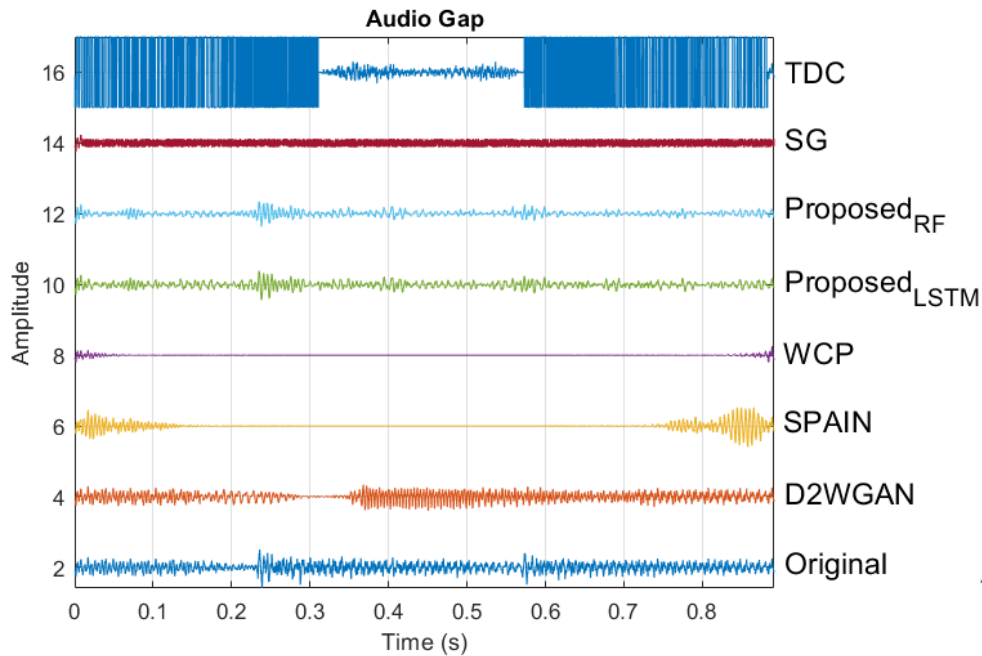


Fig. 8. A zoom-in into the reconstructed gap of Fig. 7. Notice how RF and LSTM predict the level of the amplitude despite the length of the gap (i.e., 882ms).

- [21] P. Yogarajah, J. Condell, K. Curran, P. McKeivitt, and A. Cheddad, "A dynamic threshold approach for skin tone detection in colour images," *International Journal of Biometrics*, vol. 4, no. 1, pp. 38, 2012.
- [22] J.M. Lilly, "Element Analysis: A Wavelet-Based Method for Analysing Time-Localized Events in Noisy Time Series." *Proceedings of the Royal Society A: Mathematical, Physical and Engineering Sciences* 473, no. 2200 (April 30, 2017): 20160776. <https://doi.org/10.1098/rspa.2016.0776>.
- [23] A. Chambolle and T. Pock, "A first-order primal-dual algorithm for convex problems with applications to imaging," *J. Math. Imag. Vis.*, vol. 40, pp. 120–145, 2011.
- [24] P. Combettes and J. Pesquet, "Proximal splitting methods in signal processing," *Fixed-Point Algorithms Inverse Problems Sci. Eng.*, vol. 49, pp. 185–212, 2011.
- [25] A. Adler, V. Emiya, M. G. Jafari, M. Elad, R. Gribonval, and M. D. Plumbley, "Audio Inpainting," *IEEE Trans. Audio, Speech, Lang. Process.*, vol. 20, no. 3, pp. 922–932, Mar. 2012.
- [26] C. Donahue, J. McAuley, M. Puckette, "Adversarial Audio Synthesis," In *proc. International Conference on Learning Representations (ICLR) 2019*.
- [27] T. Thiede, W. Treurniet, R. Bitto and C. Schmidmer, "PEAQ - The ITU Standard for Objective Measurement of Perceived Audio Quality", *J. Audio Eng. Soc.*, Vol. 48, No 1/2, January/February 2000.
- [28] P. Kabal, "An Examination and Interpretation of ITU-R BS.1387: Perceptual Evaluation of Audio Quality", TSP Lab Technical Report, Dept. Electrical and Computer Engineering, McGill University, May 2002.
- [29] R. Huber, and B. Kollmeier, "PEMO-Q—A new Method for Objective Audio Quality Assessment using a Model of Auditory Perception." *IEEE Transactions on Audio, Speech and Language processing*, Vol. 14, no. 6, pp. 1902 - 1911, 2006.
- [30] M. Hansen and B. Kollmeier, "Objective modelling of speech quality with a psychoacoustically validated auditory model," *J. Audio Eng. Soc.*, vol. 48(5), 395–409, 2000.